

EXPERIMENTAL STUDY ON THE COMPOSITE STEEL FRAME-RC INFILL WALL STRUCTURE

PENG Xiaotong¹ GU Qiang² LIN Chen³

¹vice-professor, School of Civil and Architectural Engineering, University of Jinan, Jinan. China

²professor, Department of Civil Engineering, Suzhou University of Science and Technology, Suzhou. China

³School of Architecture & Landscape Design, Shandong University of Art and Design, Jinan. China

Email: pengxito@163.com

ABSTRACT:

The composite steel frame-reinforced concrete infill wall structure combines advantages of both steel frames and RC infills walls and thus receives the increasing recognition in seismic areas. In order to study seismic behavior and force distribution in the structural system, the test, two-story one bay specimen under cyclic load, was performed. Based on that, the main characters such as, general behavior, local response and force distribution, were analyzed and evaluated. The experimental results indicate that the structure has adequate strength redundancy and sufficient lateral stiffness. The structural system has good performances on ductility and energy dissipation. The steel framework undertakes 80%~100% of the whole overturning moment and the infill wall takes 80%~90% of overall lateral load. Finally the design recommendations are presented.

KEYWORDS: composite steel frame, RC infill wall, seismic behavior, experiment

1. PREFACE

Since the moment-resisting steel frames have several disadvantageous problems, such as weak lateral stiffness, large deformation under horizontal loads and insufficient rotation capacity of connections under strong earthquake, the lateral resisting systems were used in practice to meet the construction requirements. The typical steel frame with resisting system is composed of two parts: the frame undertaking gravity load and the resisting system. Once steel shear walls are adopted as the resisting system, the steel plates should be thicker or stiffened for the potential of plane buckling. An alternative method is to use RC infill walls as the resisting system. The RC infill walls have the benefit of increasing the lateral stiffness dramatically, thus reducing the seismic demands on the steel frames. This provides the opportunity to use partially-restrained (PR) connections instead of more expensive fully-restrained connections. This philosophy has led to the development of the composite steel frame-RC infill wall structures (SRCW) with semi-rigid joints. In the SRCW system, steel columns and beams serve as boundary members to resist gravity loads and most of the overturning moment, while RC infill walls carry most of the shear forces. Along interfaces between steel frames and RC infill walls, the headed studs can be used to transfer shear forces uniformly to ensure effective composite interaction, as shown in Figure 1. In order to study the hysteretic behavior and put forward recommendations for earthquake-resistant design, a specimen of one-third scale was tested under cyclic load. Based on that, the seismic behavior and force distribution of this structural system were analyzed and evaluated.

2. EXPERIMENTAL PROGRAM

2.1 Specimen Design and Test Setup

The two-story, one bay specimen, which had the strong axis of steel columns oriented perpendicular to the plane

of the infill wall, was meant to represent the bottom two stories of the prototype infilled steel frame at approximate one-third scale. As shown in Figure 1, the steel columns comprised HW150X150 wide-flange shapes, while the steel beams comprised I18 hot-rolled shapes. The steel frame material was Q235 Grade B. The RC infill wall was 90mm thick, with strength Grade of the concrete targeted at C35. In the infill wall, $\Phi 8$ Grade HPB235(I) steel bars were used as horizontal bars and the corresponding horizontal reinforcement ratios were 0.895%, while $\Phi 6$ Grade HPB235(I) steel bars were used as vertical bars and the corresponding vertical reinforcement ratios were 0.505%. The confining reinforcement cages, comprising rectangular hoops and four horizontal bars, were placed all around the infill wall perimeter in the specimen. The rectangular hoop was $\Phi 4$ wire ties, arranged at 50mm spacing. Four horizontal bars ($\Phi 8$) were tied to the corners of the rectangular hoop to form the confining cage. The headed stud was 13mm in diameter and 95mm in length with 110mm spacing all around the infill wall perimeter. The PR connections comprising top and seat angles (2L140 \times 90 \times 10) and double web angles (2L63 \times 6) were used in the specimen.

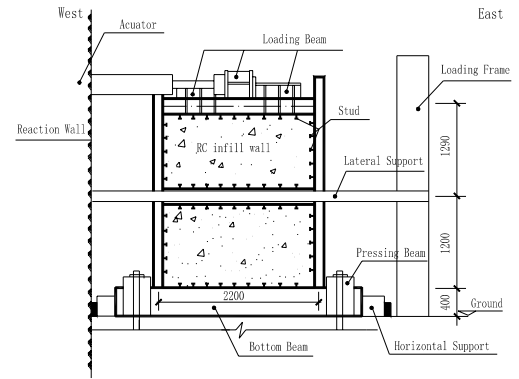


Fig.1 Test Setup

The cyclic load was applied on the loading beam placed on the top beam using two actuators with each has 100t loading capacity. Two lateral supporting beams were installed on both sides of the specimen to prevent the possibility of out-of-plane deformation. Horizontal supports and pressing-beam were anchored on the bottom beam of the specimen to strengthen restriction stiffness, thus realizing fixed restriction on the foot.

2.2 Instrumentation and Loading History

The specimen was heavily instrumented in order to obtain comprehensive strain information. Strain gages and strain rosettes were placed at critical regions (the bottom, the middle and the top) of both steel columns, partially-restrained connection regions and both ends of beams in the first story as well as second story. Two strain gages were placed on the opposite sides of the headed stud shaft and were placed as close to the stud base as possible.

Three linear position transducers (LPT) were attached to east column to measure the lateral interstory displacement. Two LPTs were placed diagonally to measure the column panel zone deformation. The behavior of the infill wall can also be represented by its diagonal deformation, which was measured by two LPTs intalled diagonally along the panel. In order to obtain the slip and separation demands of the interface studs, LPTs were arranged along the interfaces between the steel frames and RC infill walls.

The first three loading groups was controlled the peak lateral load, with 300 kN for group No.1 including 1 loading cycle, 450 kN for group No.2 including 1 loading cycle, 600 kN for group No.3 including 3 loading cycles. The remaining 2 loading groups, with each one has 3 loading cycles, was controlled by peak point drift of the specimen, with 19.4mm for group No.4, with 25.8mm for group No.5, with 32.3mm for group No.6 until the specimen was failed.

2.3 Material Properties

The material properties of the steel frames and reinforcing bars used for RC walls are reported in Table 1. the f_{cm} of concrete cube (150mm \times 150mm \times 150mm) was 46.89kN/mm², meeting design-strength of C₃₅ basically. The tensile yield strength (f_y) of the stud is 448.639N/mm², which is 0.85% of the ultimate strength (f_u). the elongation ratio (δ_s) is 4.643%.

Table 1 Material Properties of Steel Member

Location	Beam web	Column web	Column flange	angle	$\phi 4$	$\phi 6$	$\phi 8$
f_v (MPa)	316	337	310	272	563	431	371
f_u (MPa)	526	471	442	437	704	539	464
E(10^5 MPa)	2.1	2.1	2.07	2.1	2.0	2.05	2.06

3. EXPERIMENTAL RESULTS

3.1 General Performances

After No.1 loading group, a few diagonal cracks initiated on the upper corners in the RC infill wall of the second story but nothing happened to the steel frame. During No.2, 3 loading group, many more cracks formed in the infill wall of both stories. During No.4 loading group, a few more cracks formed and others progressed in the infill, and spalling of concrete occurred at upper corners of the second story. After that loading group, the rigid-displacement happened to the specimen because of insufficient stiffness of pressing-beam and improper settlement of Horizontal supports for the base, thus leading to dissymmetry of hysteretic curves. During No.5 loading group, the specimen reached its lateral ultimate strength at 928.40 kN. Meanwhile, lots of audible bangs were recorded, which was reasoned that these bangs were results of the sudden low-cycle fatigue fractures of headed studs. Moderate yielding occurred in the panel zones of the top beam-to-column connection regions. During 61 cycle of No.6 loading group, when peak lateral drift reached 32.71mm and corresponding lateral load reached 786.60 kN, the specimen started to shake heavily and the top beam was separated from the infill wall for the headed studs fractured entirely along the interfaces. More and more concrete spalled in the four corners of the second story and plastic deformation was observed at the PR connections. There was big crack occurred to the location where the vertical reinforcing cages were settled. The cracking and failure patterns were plotted in Figure 2 and the hysteretic curve was shown in Figure 3.

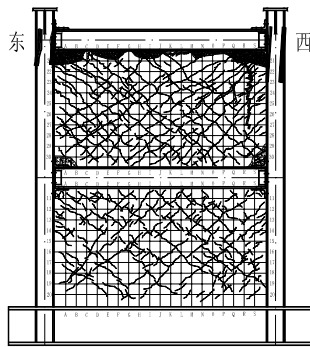


Fig.2 Cracking and Failure Patterns

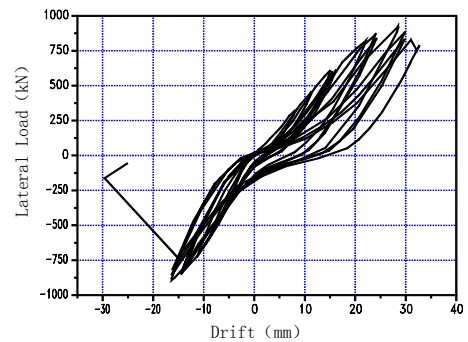


Fig.3 Total Drift versus Lateral Load curve

3.1.1 Strength and stiffness

According to Chinese relevant specifications, the lateral design strength is 295.50 kN for the specimen, close to the peak value of the first loading group. The ultimate strength (928.40kN) is about 3.11 times of the design strength, which indicates the SRCW system has ample strength bearing capacity and adequate strength redundancy.

The stiffness of the specimen was evaluated using the method of peak-peak stiffness (K_{pp}), which is the slope of the line connecting the positive and negative point of each hysteretic loop. The stiffness of every loading cycle was calculated and listed in Table 2. As seen from the table, the stiffness almost has no change for the anterior

three loading group, that means the specimen behaved elastically. The stiffness began to drop from No.4 loading group. Comparing to the initial stiffness, it decreased by 9.7% for the first cycle, 12.1% for the second cycle and 14.9% for the third cycle, taking on the phenomena of stiffness degradation. The stiffness of three cycles of No.5 loading group is decreased by 22.11%, 25.69%, and 37.34% respectively, especially the decreasing in stiffness of the third cycle is much greater, which is due to the studs' fractures in large quantity and crushing of corner concrete. The failure stiffness of the specimen is 31.73kN/mm, approximately 62.66% of the initial stiffness, thus the stiffness lose is about 40%. The interstory drift and stiffness of the first story is different from that of second one (Table 2). Before No.4 loading group, the interstory drift of the first and the second story almost have the same value, which indicates that deformation of the whole structure is varying linearly. By No.4 loading group, the drift of the second story dominate the overall structural response for the reasons that firstly, more cracks occurred to the second story than the first story and much more earlier; secondly, concrete at the corners of second story was crushed and spalled severely, while it is maintained well at the corners of first story; lastly, the constraints on first story were stronger than the second one, which caused the weaker stiffness of the second story.

Table 2 Experimental Results (Strength, Stiffness, Interstory drift)

Loading Group	Cycle	East Direction		Symbol	West Direction		Symbol	Stiffness (kN/mm)	Δ_1/Δ (%)		Δ_2/Δ (%)	
		Drift (mm)	Reaction Force(kN)		Drift (mm)	Reaction Force(kN)			$+\Delta_1/\Delta$	$-\Delta_1/-\Delta$	$+\Delta_2/\Delta$	$-\Delta_2/-\Delta$
1	1	8.12	323.80	11	-4.68	-324.40	-11	50.64	52.71	40.60	47.29	59.40
2	1	11.30	457.40	21	-6.78	-455.80	-21	50.54	50.62	42.77	49.38	57.23
3	1	15.03	609.20	31	-9.08	-608.60	-31	50.53	48.50	42.29	51.50	57.71
	2	15.47	600.20	32	-9.47	-631.00	-32	49.39	48.03	42.20	51.97	57.80
	3	16.19	610.60	33					46.40		53.60	
4	1	22.02	819.00	41	-14.47	-849.60	-41	45.74	44.50	41.67	55.50	58.33
	2	24.08	872.40	42	-13.74	-811.60	-42	44.54	40.45	43.09	59.55	56.91
	3	24.24	839.00	43	-13.80	-799.60	-43	43.08	40.02	42.75	59.98	57.25
5	1	28.50	928.40	51	-16.33	-890.80	-51	39.44	39.44	42.80	60.56	57.20
	2	29.84	883.20	52	-16.36	-855.40	-52	37.63	37.40	41.20	62.60	58.80
	3	29.76	832.20	53	-16.20	-816.40	-53	35.87	36.56	40.25	63.44	59.75
6	1	32.71	786.60	61	-15.15	-731.80	-61	31.73	35.19	36.26	64.81	63.74

31 (-31):1/4 cycle of No.3 loading group in east(west) direction; Δ_1 : interstory drift of 1 story; Δ_2 : interstory drift of 2 story; Δ :overall drift; -33 was not recorded.

3.1.2 Ductility and energy dissipation

The ductility coefficient μ ($\mu = \delta_u / \delta_y$) and relative deformation ratio are adopted to evaluate the ductility. As shown in Table 2, the stiffness began to decrease obviously from No.4 loading group, therefore the second cycle of No.3 loading group is taken as the end of elastic stage, thus $\delta_y = 15.47\text{mm}$ and corresponding F_y is 600.2kN. The δ_u ($\delta_u = 32.71\text{mm}$), which is taken from the displacement corresponding to the 85% ultimate load ($84.7\% \times 928.4 \text{ kN} = 786.6 \text{ kN}$) in the range of descending stage of envelope line of hysteretic curve, is close to peak displacement of the first cycle of No.6 loading group.

The ductility coefficient (μ) and relative deformation ratios are calculated in Table 3, indicating that the ductility coefficient of the second story (2.64) was more than 1.7 times than that of the first story and 1.25 times

than that of integral structural system. Since heavy constraints were imposed on the bottom of the first story, the ductile capacity of first story was less than second one. But in real practice, this effect is most likely ignored because that many building have a taller first story and the foundations usually allow some deformation to a certain degree.

Table 3 Ductility and Displacement Capability

Location	δ_y (mm)	δ_u (mm)	Height (mm)	Ductility Coefficient (μ)	Deformation Ratio δ_u/H (%)
1 Story	7.43	11.51	1200	1.55	0.96
2 Story	8.04	21.20	1290	2.64	1.64
Overall	15.47	32.71	2490	2.11	1.31

The energy dissipation ratios (W_r) are used to describe energy dissipation capacity. According to the experimental load-displacement curves, area of every hysteretic loop in the first quarter-quadrant A_i is calculated. divide A_y ($A_y = F_y \times \delta_y = 600.2 \text{ kN} \times 15.47 \text{ mm}$) to obtain energy dissipation ratio ($W_{ri} = A_i / A_y \times 100\%$) of each loading level (Table 4). The structural system had a better energy dissipation capacity and the maximum energy dissipation ratio reached 84.72%. There was almost no energy absorbed in the first two loading group and the energy dissipation ratio was less than 10%, indicating that the specimen still behaved in elastic stage. During No.4 loading group, the specimen had a great increase in energy dissipation through massive cracks formed in the infill wall, rotation of the connections, yielding of angles and steel members and fracture of the studs. The increasing amount of yielding in steel members, together with crushing and spalling of the corner concrete, are considered to have contributed to the continuous increase in energy dissipation during No.5, 6 loading group.

Table 4 Energy Dissipation

Loading Group	1Story W_{r1}	2Story W_{r2}	Overall W_{ro}	W_{r1} / W_{ro}	W_{r2} / W_{ro}
1	3.41	2.77	6.18	55.24	44.76
2	4.76	3.90	8.66	54.93	45.07
3	8.04	10.65	18.69	43.02	56.98
4	16.90	23.50	40.40	41.84	58.16
5	30.63	42.85	73.48	41.69	58.31
6	30.39	54.34	84.72	35.86	64.14

3.2 Local Behavior

3.2.1 Internal forces of steel columns

The Overturning moment was resisted by the mutual action of tensile columns and compressive columns, thus the axis forces were getting smaller along height of the columns for the overturning moment was reduced continuously. At the bottom of columns, the axis force of compressive column was lower than that of tensile column. This phenomenon was due to the fact that, when the column was in compression, the infill wall around the column was pressed closely so that some parts of concrete participate in resisting the overturning moment leading to decreases in compressive force of columns; whereas, the concrete around the tensile column was lack of the united action so that the contribution of concrete to tensile columns was smaller, consequently the neutral axis formed by the two columns moved to the compressive end. In reverse loading, the favorable effect to

compressive column (primary tensile column) caused by concrete appeared to decline because that the united action was getting weaker for the incompatible deformation pattern.

3.2.2 Partially restrained connections

The Rotation and elongation of connections were calculated based on the readings of two LPTs placed horizontally. The PR connections were very stiff in rotation for early loading groups (No.1, 2) due to restraints from the concrete. The connections started to rotate from No.3 loading group and the rotation value was 0.003rad on 31 cycles. During No.4 loading group, the rotation increased 1 time than last loading group, reached 0.006rad. The maximum rotation of connection reached 0.0115rad abruptly at 61 cycle. With increasing of the rotation of beam ends, the bending moment of beam ends had a decreasing tendency contrarily, for the reasons that during 11 cycle, the bending moment varied linearly with the rotation for the connections were confined by the concrete; At the end of 21 cycle, the connections lost restraints from concrete to some extent, and there was a gap (12mm) between columns and beams, lastly the thickness of beam and column flange was larger than that of the horizontal legs of the angles, so that the rotation was mainly composed of deformation of the angles and the ends of the beam only had rigid movement; During 51 cycle, since less constraints on the corner region, the angles could deform more freely resulting in the corresponding decreases in the bending moment of beam ends. Therefore, it can be concluded that once the corner concrete of infill walls was failed and the composite action was deteriorated, the Partially Restrained Connections play an important role in resisting overturning moment and ensure integrity of the whole structure.

3.2.3 Headed studs

Almost every stud along the interfaces between steel frame and infill wall was monitored. The results show that except for the studs located in the middle region, all the others were yielded or fractured; especially the studs along the upper interface of second story were fractured totally, as shown in Figure 4. Sections of the failed studs were smooth and glossy, and the failure deformation value was less than that of the previous load cycle. These phenomena show that the studs were failed due to low-cycle fatigue. The failure sequence of the studs can be described as follows: studs at corners of the upper interface of the second story began to yield and extend to the center; then studs at the lower corners of the first and second story's western interfaces and those at the west corners of the first story's upper interface yielded and progressed to the middle areas; and then studs at the east corners of the lower interface of the second story and on the east interface yielded uniformly; studs on the west surface of the lower interface of the second story yielded eventually. The main function of studs is to transfer shear forces uniformly between steel frames and infill walls to ensure effective composite interaction. The studs carried not only shear forces but also axial forces due to the deformation incompatibility between the steel frame and infill wall. The surrounding concrete could disperse pressure of the studs, so the studs were under the interaction of tension and shear mainly. Comparative analysis of axial strain and bending strain of studs at different positions was carried out aiming at understanding the shear resisting capacity of studs under tensile forces. It shows that the shear forces that studs endured along the same interface was consistent basically because of the mutual connection of confining cages in the infill wall, which ensure the shear forces distributed uniformly. The studs at the corners carried tensile forces mostly for the concrete there was ripped and crushed. As to the studs at the horizontal interfaces, the closer to base of the specimen the smaller shear forces the studs endured, because more and more shearing forces was shared by



Fig 4 Fractured Studs on Upper Interface of Second Story

frame columns.

3.3 Force Transfer Mechanism

3.3.1 Lateral force distribution

As shown in Figure 5, the lateral load transferred to the base by three ideal routes: transferred between infill wall and steel frame through studs; transferred down by the diagonal compression struts in the RC infill walls; transferred by the steel frame alone through deformation. The experimental results show that during 11 cycle, studs at section B carried 75% of the total lateral forces, and the proportion increased gradually with the increasing of lateral load. The maximum percentage of lateral load that studs undertaken reached 85%. Studs at section C resisted approximately 87% of total lateral forces, where studs at section E underwent the largest percentage of lateral load at 90%, whereas the smallest percentage of lateral load was 83%. In sum, the studs (infill wall) take 80%~90% of the total lateral load; The steel frames share 10%~20% of the total lateral load indicating that the steel frames carry the lateral load in certain quantities from the very beginning.

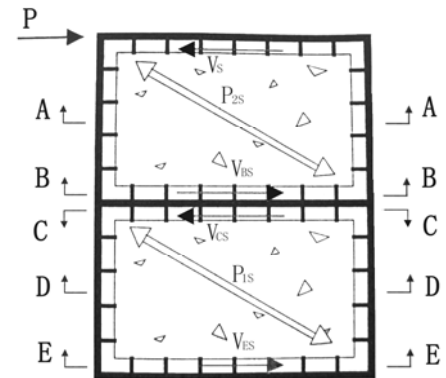


Fig 5 Lateral Shear Force Transfer Mechanism

3.3.2 Distribution of overturning moment

The percentage of the overturning moment (section E) resisted by steel frames increased from 78.3% at 11 cycle to 99% at 31 cycle; and the percentage of section D was stable at 95% or so.

4. CONCLUSIONS AND DESIGN RECOMMENDATIONS

The SRCW structural system has multiple lateral force transfer routes: the interaction between studs and infill walls; the diagonal compression strut between steel frames and infill walls; the self-resist ability of the steel frames against lateral load. Therefore, the structure has ample lateral bearing capacity and adequate strength redundancy.

The concrete infill wall could provide the sufficient lateral stiffness for the structure, which confine the lateral drift in an allowed range and reducing the seismic demands on the steel frames. This provides the opportunity to use PR connections, which enhance the ductility and avoid the abrupt decrease in strength and stiffness after the infill wall was failed.

The structural system has a good energy dissipation capacity. It could absorb energy through cracking in the infill walls, friction effects of aggregates on the cracking interface, rotation of the connections, yielding of angles and steel members, fracture of the studs, together with crushing and spalling of the concrete.

The composite interactions of the structure are achieved by the headed studs, which transfer the shear forces between the steel frames and infill walls. The existence of studs makes the infill wall become a series of diagonal struts and later deteriorate into one catercorner strut with continuous fracture of the studs, therefore the composite interaction is getting weaker. Eventually, with crushing of the catercorner strut, the composite interactions of the SRCW structure come to an end.

The majority of overturning moment was resisted by the steel frames with the percentage about 80%~100%, and the percentage that the infill wall undertaken is about 10%~20%; the most of lateral load was resisted by the studs (infill wall) with the percentage about 80%~100%, the percentage that the steel frames undertaken is

about 10%~20% and the percentage that the diagonal strut transferred is about 10%~15%. The design methods proposed by the document [2] are described as follows: The steel frames resist 100% of the overturning moment and the moment-resist capability of the infill wall (shear wall) is ignored. This design principle is feasible and has a certain safety factor for the steel frames, but it is unsafe for the shear wall; the design principle, the shear infill wall resist all the lateral force and neglect the helpful effects of steel frames, is safer for the infill walls but insecure for the steel frames.

The studs play an important role in the SRCW structure. Its strength, quantity, and layout position have a direct impact on performances of the structure. In general, increasing the horizontal studs is a good way to improve the energy dissipation capacity of the structure. In designing the studs, the effect of axial tensile forces on the shear strength should be taken into account, therefore the shear strength of the studs should be cut down to an appropriate degree. Some necessary measures should be taken to enhance the fatigue life of studs in the construction.

The partially restrained connections should be adopted in the SRCW structure instead of rigid connections, because the decreasing in stiffness of connections would improve the ductility and energy dissipation capacity of the structure.

REFERENCES

- [1] Peng Xiaotong. (2006). Hysteretic behavior and design criterion of composite steel frame-reinforced concrete infill wall structural system [D]. Xi'an: Xi'an University of Architecture and Technology
- [2] Xiangdong Tong, Jerome F. Hajjar, Arturo E. Schultz, Carol K. Shield. (2005). Cyclic behavior of steel frame structures with composite reinforced concrete infill walls and partially-restrained connections. *Journal of Constructional Steel Research* **61**, 531–552
- [3] Makino M., Kawano A., Kurobane Y., Saisho M. and Yoshinaga K. (1980). An investigation for the design of framed structures with infill walls. *Proceedings of the Seventh World Conference on Earthquake Engineering, Istanbul, Turkey*, **4**, 369-372.
- [4] Hayashi M. and Yoshinaga K. (1985). An experimental study of practical application of composite structures of a frame and an earthquake-resistant wall1. *Synopses of the Conference of Architecture Institute of Japan, AIJ, Tokyo, Japan*, 1335-1336.
- [5] Hayashi M. and Yoshinaga K. (1987). An experimental study of practical application of composite structures of a frame and an earthquake-resistant wall3. *Synopses of the Conference of Architecture Institute of Japan, AIJ, Tokyo, Japan*, 1317-1318.